Structure of 7-Azaindole···2-Fluoropyridine Dimer in a Supersonic Jet: Competition between N–H···N and N–H···F Interactions

ARTICLE *in* THE JOURNAL OF PHYSICAL CHEMISTRY A · AUGUST 2011

Impact Factor: 2.69 · DOI: 10.1021/jp205894q · Source: PubMed

4 AUTHORS:

Sumit Kumar
Indian Institute of Science Education and Re…
9 PUBLICATIONS **72** CITATIONS
SEE PROFILE

Indu Kaul
Indian Institute of Science Education and Re…
4 PUBLICATIONS **27** CITATIONS
SEE PROFILE

Partha Biswas
Scottish Church College
12 PUBLICATIONS **66** CITATIONS
SEE PROFILE

Aloke Das
Indian Institute of Science Education and Re…
34 PUBLICATIONS **246** CITATIONS
SEE PROFILE

THE JOURNAL OF PHYSICAL CHEMISTRY A

ARTICLE

pubs.acs.org/JPCA

Structure of 7-Azaindole···2-Fluoropyridine Dimer in a Supersonic Jet: Competition between N−H···N and N−H···F Interactions

Sumit Kumar, Indu Kaul, Partha Biswas,[†] and Aloke Das*

Department of Chemistry, Indian Institute of Science Education & Research (IISER), 900 NCL Innovation Park, Dr. Homi Bhabha Road, Pune-411008 Maharashtra, India

Supporting Information

ABSTRACT: In the present work, we have investigated the structure of 7-azaindole···2-fluoropyridine dimer in a supersonic jet by employing resonant two photon ionization (R2PI), IR-UV, and UV−UV double resonance spectroscopic techniques combined with quantum chemistry calculations. The R2PI spectrum of the dimer is recorded by electronic excitation of the 7-azaindole moiety, and a few low frequency intermolecular vibrations of the dimer are clearly observed in the spectrum. The electronic origin band of the dimer is red-shifted by 1278 cm^{-1} from the $S_1 \leftarrow S_0$ origin band of 7-azaindole monomer. The presence of a single conformer of the dimer is confirmed by IR-UV and UV−UV hole-burning spectroscopic techniques. RIDIR (Resonant ion dip infrared) spectrum of the dimer shows a red-shift of 265 cm^{-1} in the N−H stretching frequency with respect to that of the 7-azaindole monomer. Two planar double hydrogen bonded cyclic structures of the dimer have been predicted from DFT calculations. Comparison of experimental and theoretical N−H stretching frequencies confirms that the observed dimer is stabilized by N−H···N and C−H···N hydrogen bonding interactions. The less stable conformer with N−H···F and C−H···N interactions are not observed in the experiment. The competition between N−H···N and N−H···F interactions in the two dimeric structures are discussed from natural bond orbital (NBO) analysis. The current results demonstrate that fluorine makes a hydrogen bond of intermediate strength through cooperative interaction of another hydrogen bond (C−H···N) present in the dimer, although fluorine is believed to be very weak hydrogen bond acceptor.

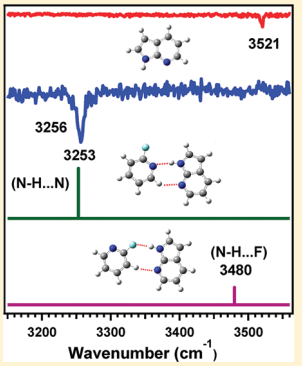

1. INTRODUCTION

Hydrogen bonding interaction is ubiquitous due to its three unique properties namely directionality, specificity, and transience.[1−3] This noncovalent interaction has immense significance in providing a specific shape of biomolecules, which is responsible for appropriate biological functions in living systems.[3−7] Hydrogen bonding interaction also plays a key role in molecular recognition, crystal structure, self-assembly, and supramolecular chemistry.[8−15] Consequently, there are extensive theoretical as well as experimental studies in the gas phase to understand this intermolecular interaction in detail.[16−19] A conventional hydrogen bond is defined as X−H···Y, where both X and Y are electronegative atoms (i.e., O, N, and F). However, it has been found that covalently bound fluorine (F) is a poor hydrogen bond acceptor in spite of its highest electronegativity.[20] Very weak hydrogen bond formation ability of fluorine has been explained in terms of its low proton affinity.

The existence of weak C−F···H−X (X = C, N, and O) hydrogen bonding interactions has first been reported by Shimoni et al. from their extensive analysis of the crystallographic data collected in the Cambridge Structural Database (CSD).[21] They have reported that though hydrogen bonding interactions through fluorine are quite weak, these are important in molecular packing in complexes and crystals. Later, Desiraju and co-workers have rigorously investigated the role of C−H···F interactions in the crystal structures of partially fluorinated benzenes.[22] They have demonstrated that C−H···F interactions are as important as C−H···O and C−H···N hydrogen bonding interactions in stabilizing crystal structures.

On the other hand, hydrogen bonding interactions through the fluorine atom have been investigated in the gas phase in the complexes of H_2O, CH_3OH, and NH_3 with a series of partially fluorinated benzenes by experimental as well as computational methods.[23−30] It has been found experimentally as well as theoretically that the most stable conformer of the complexes of both H_2O and CH_3OH with partially fluorinated benzenes has an in-plane six-membered cyclic structure with O−H···F and C−H···O double hydrogen bonding interactions. Tonge et al. have studied the 1:1 complex of fluorobenzene and ammonia by experimental as well as high level theoretical calculations.[30] They have confirmed that the most preferred conformation of the complex has an in-plane six-membered cyclic structure with N−H···F and C−H···N double hydrogen bonding interactions, which are analogous to fluorobenzene···H_2O and fluorobenzene···CH_3OH structures. On the contrary, Vaupel et al. have reported a N−H···π bound structure for fluorobenzene···NH_3 complex and σ-type N−H···F hydrogen bonded structure for difluorobenzene···NH_3 complex.[26] Recently, Singh et al. have performed theoretical investigation of

Received: June 23, 2011
Revised: August 7, 2011
Published: August 11, 2011

dx.doi.org/10.1021/jp205894q | J. Phys. Chem. A 2011, 115, 10299–10308

hydrogen bonded complexes of NH_3 with a series of partially fluorinated benzenes.[31] They have found that 1:1 complexes of NH_3 with fluorobenzene, difluorobenzene, and trifluorobenzene prefer in-plane cyclic structure with C−H···N−H···F−C motif. They have also demonstrated that the absence of an exclusively in-plane linear N−H···F hydrogen bond in the complexes of NH_3 with fluorinated benzenes is due to the very weak hydrogen bond formation ability of the fluorine atom. Rather, the stability of these cyclic complexes is due to cooperativity of the two hydrogen bonds, C−H···N and N−H···F.

Although fluorine is a weak hydrogen bond acceptor, participation of fluorine in the hydrogen bonding interaction is controversial. To understand the importance of hydrogen bonding interaction in stabilization of Watson−Crick base pairs in the double helical structure of DNA, several studies are performed with modified nucleobases, where the N−H or C═O hydrogen bonding groups are replaced by nonpolar C−H or C−F groups.[32−38] It has been found that these modified nucleobases show surprising base pair stability and even selective replication by DNA polymerases. On the basis of this observation, Kool and others have claimed that the structure of DNA is stabilized even if it lacks hydrogen bonding interaction and the stability is due to π-stacking interaction only.[39,40] However later, it has been established by NMR and computational studies that the unexpected stability of fluorine-substituted base analogs in DNA is due to C−H···F, N−H···F, and C−H···N hydrogen bonding interactions.[41−43] The surprisingly high binding affinity of 2′-fluoroarabinonuleic acid (2′F-ANA) compared to arabinonuleic acid (ANA) to DNA and RNA has been demonstrated by Anzahaee et al. in terms of the C−H···F−C hydrogen bonding interaction.[44] To determine the intrinsic intermolecular interactions responsible for the stability of the base pairs containing fluorine-substituted base analogs, Leutwyler and co-workers have studied the complexes of nucleobase mimic 2-pyridone and a series of substituted fluorobenzenes in the gas phase.[45−47] From their experimental as well as theoretical studies, they have reported that mono- to pentafluorobenzene complexes of 2-pyridone form only doubly hydrogen bonded dimers through N−H···F−C and C−H···O═C interactions. Only the complex of hexafluorobenzene and 2-pyridone forms a π-stacked dimer.

In this study, we have investigated the structure of the 7-azaindole···2-fluoropyridine (7-AI···2-FP) dimer in a supersonic jet by using resonant two photon ionization (R2PI), infrared−ultarviolet (IR-UV), and ultraviolet−ultraviolet (UV−UV) double resonance spectroscopic techniques as well as quantum chemistry calculations. There are possibilities of two double hydrogen bonded structures of the dimer, one with N−H···N and C−H···N interactions and the another with N−H···F and C−H···N interactions. As fluorine is a weak hydrogen bond acceptor, it is expected that the N−H···N interaction unfavorably competes with the N−H···F interaction in the dimer. However, due to the cooperativity of hydrogen bonded network, the N−H···F hydrogen bond could be strengthened due to the presence of the C−H···N interaction in the doubly hydrogen bonded dimer. The aim of the current investigation is to determine the structure of the 7-AI···2-FP dimer in the gas phase as well as the competition between N−H···N and N−H···F interactions in the dimer. As 7-azaindole is a model system for the nucleic acid base adenine, the study of double hydrogen bonded complex of 7-azaindole also sheds light on the hydrogen bonding characteristics of the nucleic acid base pair. Thus, not surprisingly, there are extensive studies on photophysics and spectroscopy of the 7-azaindole dimer and its hydrogen bonded complexes in the literature.[48−63] The current report focuses on the hydrogen bonding characteristics of the 7-AI···2-FP heterodimer, which especially mimics the interaction between a model nucleic acid base and fluorinated aza-aromatic system known as a modified nucleic acid base analog.

2. METHODS

2.1. Experimental Section. The experimental setup to measure jet-cooled resonant two photon ionization (R2PI) as well as IR/UV double resonance spectra has been described in detail elsewhere and mentioned here briefly.[64] 7-Azaindole (7-AI) was put in a stainless steel sample holder placed behind a pulsed valve and heated at about 95 °C. The buffer gas argon at a pressure of about 45 psig was bubbled through 2-fluoropyridine (2-FP) taken in a stainless steel sample container maintained at 0 °C and kept outside the vacuum chamber. 2-FP (Sigma Aldrich) vapor seeded in the buffer gas was mixed with 7-AI (Sigma Aldrich) vapor and expanded into the vacuum through a 0.5 mm pulsed nozzle (General valve, series 9, rep. rate 10 Hz). Jet-cooled 7-AI monomer as well as 7-AI···2-FP mixed dimer were ionized using one-color resonant two photon ionization (1C-R2PI) technique by frequency doubled output of a tunable dye laser (ND6000, Continuum) pumped by the second harmonic of a Nd:YAG laser (nanosecond, 10 Hz, Surelite II-10, Continuum). The resolution of the dye laser is about 0.08 cm^{-1}. Typical UV pulse energy used for ionization was about 0.4−0.5 mJ. The ions were mass analyzed in the time-of-flight mass spectrometer and detected by a 18 mm diameter dual MCP detector (Jordan TOF Products) placed at the end of the time-of-flight tube. The ion signal from the detector was amplified using a preamplifier (SRS, Model SR445A) and sent to a digital oscilloscope (Tektronix, 350 MHz, DPO 4034) interfaced to a PC via a USB port. Both data acquisition and laser control were performed using home-built LabView (National Instruments, 8.6 Version) based programs.

IR spectra of the 7-AI monomer and 7-AI···2-FP dimer were measured using resonant ion dip infrared spectroscopy (RIDIRS). In this technique, two counter-propagating IR and UV laser beams were spatially overlapped and intersected the molecular beam at a right angle. The typical pulse energy of the IR laser beam used was about 4−5 mJ, and it was focused using a CaF_2 lens of focal length 185 cm, whereas the UV laser beam used was unfocused and the typical energy was about 0.4 mJ. IR laser, which was fired about 100 ns prior to the UV laser, was scanned through the vibrational transitions in the ground electronic state while the UV laser was fixed to a particular transition in the R2PI spectrum of the dimer. Thus IR spectra were obtained as a depletion of the ion signal, whenever the IR laser frequency was matching with any vibrational transition of the complexes in the ground electronic state.

IR−UV and UV−UV hole-burning spectroscopic techniques were used to discriminate the transitions in the R2PI spectrum, which belong to different conformers. IR-UV hole-burning spectroscopic technique is just opposite to RIDIRS. Here the IR laser was kept fixed at a particular vibrational frequency of a conformer and the UV laser, which was fired after 50−100 ns from the IR laser, was scanned through the R2PI spectrum. As the IR laser would burn the population of a specific conformer through vibrational excitation, the UV excitation peaks of that conformer would show reduced intensity compared to those in the R2PI spectrum. On the other hand, the intensity of the UV

excitation peaks of the other conformers in the R2PI spectrum would be unaltered even in the presence of the IR beam. In UV−UV hole-burning spectroscopic technique a relatively high powered UV laser (hole-burning laser, 10 Hz, pulse energy 0.4−0.5 mJ) is scanned through the wavelength region of the R2PI spectrum of the molecule. A second UV laser (probe laser, 10 Hz, pulse energy 0.2−0.3 mJ) fired 50−100 ns after the hole-burning laser is spatially overlapped with the first laser and kept fixed at particular transition in the R2PI spectrum. All vibronic transitions arising from the same ground state will show depletion in the hole-burning spectrum. The tunable IR laser was a KTA based OPO (Laser Vision) pumped by an unseeded Nd:YAG laser (ns, 10 Hz, Surelite II-10). Typical resolution of the IR laser used in the experiment is about 2−3 cm^{-1}. Temporal synchronization among the pulsed valve and various lasers was controlled by using a digital delay generator (BNC, Model 575).

2.2. Computational Section. Ground state geometry optimization and harmonic vibrational frequency calculations of two possible double hydrogen bonded conformers of the 7-AI···2-FP dimer were performed at the density functional level of theory (DFT) using 6-311++G(d,p) and aug-cc-pVDZ (aVDZ) basis sets. Various functionals like B3LYP, PW91, and M05-2X were used for the DFT calculations using "ultrafine" numerical integration grid. The binding energies of various conformers of the dimer were corrected for basis set superposition error (BSSE) and zero-point vibrational energy (ZPE). BSSE correction was done using the counterpoise method given by Boys and Bernardi.[65] Natural bond orbital (NBO) analysis for different conformers of the dimer was performed to determine the strength of the hydrogen bonding interactions present there.[66,67] NBO pictures of various conformers of the dimer have been obtained using NBO View (Version 1.1) software.[68] Excited state geometry optimizations and frequency calculations of the monomer and the mixed dimer were done at the CIS/6-31++G(d,p) level. All calculations were performed using Gaussian 03 program package.[69]

3. RESULTS AND DISCUSSION

3.1. Resonant 2-Photon Ionization (R2PI) Spectra. Figure 1b shows one-color R2PI spectrum recorded in 7-AI···2-FP dimer mass channel at 215 am.u. One-color R2PI spectrum of the 7-azaindole monomer is shown in Figure 1a to compare with the dimer R2PI spectra. The origin band (0_0^0) for the $S_1 \leftarrow S_0$ electronic transition of 7-azaindole appears at 34637 cm^{-1}, which matches well with the previous reports.[52,53,70] The R2PI spectrum of the 7-AI···2-FP dimer is measured by electronic excitation of the 7-azaindole moiety. The lowest energy and most intense band observed at 33359 cm^{-1} in the spectrum has been assigned as the $S_1 \leftarrow S_0$ origin of the dimer, and it is red-shifted from the electronic origin band of 7-azaindole monomer by 1278 cm^{-1}. The R2PI spectra of both monomer and dimer have been recorded up to 1000 cm^{-1} above the S_1 origin and shown in relative wavenumber scales, which are relative to the respective electronic origin bands at 34637 and 33359 cm^{-1}. Lin et al. have previously assigned the vibronic bands of 7-azaindole monomer according to Mulliken's notation and the same assignment scheme has been followed here for the assignment of the intramolecular vibrations observed in 7AI···2-FP dimer.[70]

The intramolecular vibrations of the 7-azaindole moiety in the dimer have been clearly identified by comparing the R2PI spectra of the monomer and the dimer depicted in Figure 1. Most of the intramolecular vibrations of 7-azaindole appear in the dimer but

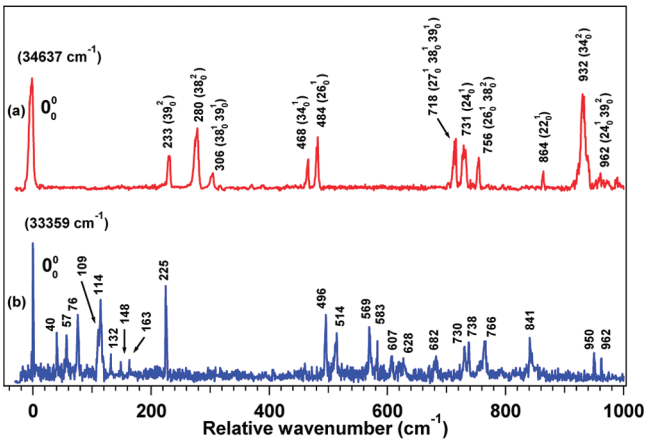

Figure 1. One-color R2PI spectra of (a) 7-azaindole monomer and (b) 7-azaindole···2-fluoropyridine dimer. The spectra have been shown in relative wavenumber scale with respect to the electronic origin bands of the monomer and the dimer. The dimer spectrum is magnified by 50 times.

with little variation in frequency as well as intensity due to formation of the double hydrogen bonded complex with 2-fluoropyridine. The two prominent intramolecular vibrations, 38_0^2 and $38_0^1 39_0^1$, of the monomer completely disappear in the dimer spectrum shown in Figure 1b. This is probably due to the reason that mode 38 is severely affected by the complex formation. Modes 39 and 38 are butterfly and ring twisting vibrations of 7-azaindole, respectively. Similarly, there is marked decrease in the intensity of the 34_0^2 vibration (950 cm^{-1}) in the dimer compared to the monomer though the intensity of the 34_0^1vibration (496 cm^{-1}) in the dimer is not affected. Mode 34 is out-of-plane NCC bending vibration of the pyrrole ring of 7-azaindole and it involves significant displacement of the nitrogen atom of the pyrrole ring. We observe here that intermolecular hydrogen bonding does not affect one quantum excitation in the mode 34 but two quanta excitation in this mode is affected. Detailed assignment of the observed intramolecular vibrations of the 7-azaindole moiety in the dimer has been discussed in the Theoretical Results section. The effect of intermolecular vibrations present in the dimer on the intramolecular modes of the excited 7-azaindole monomer moiety in the dimer has been reported recently for the 7-azaindole···formamide dimer.[63]

Specific types of low frequency intermolecular vibrations are very often observed in the electronic spectrum of the dimer, especially when they are double hydrogen bonded.[45] The remaining bands apart from the assigned intramolecular vibrations of the excited monomer unit (7-azaindole) of the dimer observed in Figure 1b could be due to either low frequency intermolecular vibrations or the presence of isomeric structures of the dimer. But IR−UV and UV−UV double resonance experiments described in the latter sections of the experimental results confirm the presence of only one conformer of the dimer in the experiment. Thus the low frequency vibrations at 40, 57, 76, 109, 114, 132, 148, and 163 cm^{-1} built off the S_1 origin of the dimer are assigned as fundamentals, overtones, and combinations of intermolecular vibrations of the dimer due to stretching and bending motions of the intermolecular hydrogen bonds. It is interesting to note that a few of these intermolecular vibrational modes also arise on the intramolecular vibrations (34_0^1, 26_0^1) of the 7-azaindole moiety of the dimer. To assign these low frequency vibrations of the dimer, S_1 state frequency calculation of the dimer has been performed.

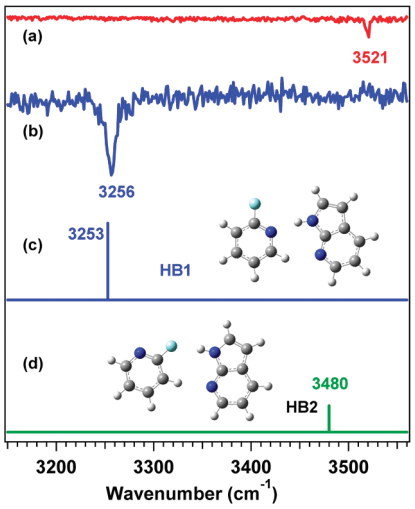

Figure 2. RIDIR spectra in the N−H stretching region by probing the origin bands of (a) the 7-azaindole monomer and (b) the 7-azaindole···2-fluoropyridine dimer. Theoretical IR spectra for HB1 and HB2 structures of the 7-azaindole···2-fluoropyridine dimer obtained at the B3LYP/aVDZ level of theory are provided in panels c and d, respectively.

We have discussed the assignment of the intermolecular vibrations in detail in the Theoretical Results section and provided the assignment in Table 4.

3.2. RIDIR Spectra. To determine the structure of the 7-AI···2-FP dimer observed in the experiment, IR spectra have been recorded by probing several transitions in the R2PI spectrum of the dimer. RIDIR spectrum provided in Figure 2a shows the N−H stretching frequency of 7-azaindole monomer at 3521 cm^{-1}, which is in good agreement with the previous report.[55] Figure 2b shows RIDIR spectrum obtained by probing the 0_0^0 band of 7-AI···2-FP dimer. The single peak observed at 3256 cm^{-1} in the dimer RIDIR spectrum is assigned to the N−H stretching vibration of the dimer, which is red-shifted by 265 cm^{-1} from that of the 7-azaindole monomer. It is interesting to compare the intensity and width of the N−H stretching peak in the 7-azaindole monomer and the 7-AI···2-FP dimer. The fwhm of the N−H stretch peak in the monomer and the dimer are 3.5 and 10 cm^{-1}, respectively. The amount of the red-shift in the N−H stretching frequency as well as significant enhancement of the intensity and broadening of the peak shown in Figure 2b compared to those for the monomer indicate the presence of strong hydrogen bonding interaction in the dimer.

Figure 2, panels c and d, presents theoretical IR spectra of two probable hydrogen bonded structures of the dimer (see Figure 6) calculated at the B3LYP/aVDZ level of theory. The calculation shows that theoretical N−H stretching frequencies of HB1 and HB2 structures of the dimer are 3253, and 3480 cm^{-1}, respectively after using a scaling factor of 0.9628. The scaling factor is obtained by taking the ratio of experimental and theoretical N−H stretching frequencies of 7-azaindole monomer obtained at 3521 and 3657 cm^{-1}, respectively. Both HB1 and HB2 conformers of the dimer have double hydrogen bonded structures but the former one with N−H···N and C−H···N interactions and the latter one with N−H···F and C−H···N interactions. The optimized geometries of HB1 and HB2 conformers are also shown in Figure 2, panels c and d. Excellent agreement between experimental and theoretical N−H stretching frequency of HB1 conformer confirms that the observed dimer has double hydrogen bonded structure with N−H···N and C−H···N interactions.

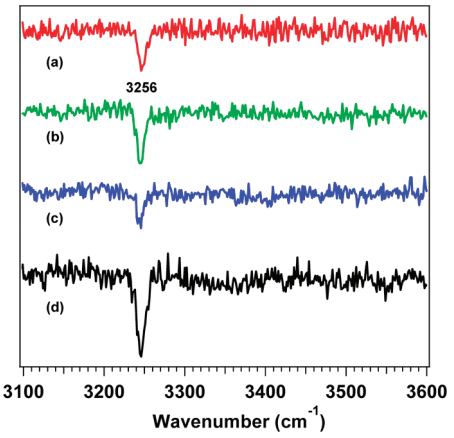

Figure 3. RIDIR spectra in the N−H stretching region by probing (a) 0_0^0 band, (b) 0_0^0 + 76 cm^{-1}, (c) 0_0^0 + 496 cm^{-1}, and (d) 0_0^0 + 766 cm^{-1} bands of the 7-azaindole···2-fluoropyridine dimer.

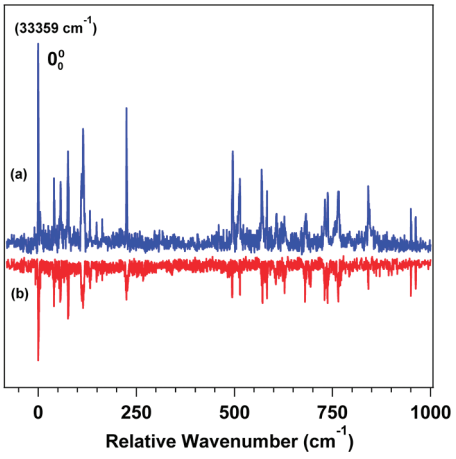

Figure 4. (a) One-color R2PI spectrum of the 7-azaindole···2-fluoropyridine dimer, and (b) UV−UV hole-burning spectrum by probing the electronic origin band of the 7-azaindole···2-fluoropyridine dimer.

It is worth comparing the N−H···N interaction present in the 7-AI···2-FP dimer with that in 7-azaindole···(NH_3)[56] and indole···(pyridine)[64] complexes. The amount of red-shift in the X-H stretching frequency in the complex generally measures the strength of the hydrogen bond. The red-shifts in the N−H stretching frequency in 7-azaindole···(NH_3), indole···(pyridine), and 7-azaindole···2-fluoropyridine complexes are 295, 257, and 265 cm^{-1}, respectively. Similar amount of red-shift in the N−H stretching frequency in all the three cases indicate that the strength of N−H···N hydrogen bonding interaction is similar in all the three complexes. RIDIR spectra have also been recorded by probing most of the intermolecular as well as intramolecular vibrations in the dimer and identical IR spectra like the one observed in Figure 2b have been obtained in every case. Figure 3b−d shows a few selected RIDIR spectra by probing the bands at 0_0^0 + 76, 0_0^0 + 496, and 0_0^0 + 766 cm^{-1} in the R2PI spectrum of the dimer. RIDIR spectrum by probing the origin band of the dimer is presented in Figure 3a for comparison.

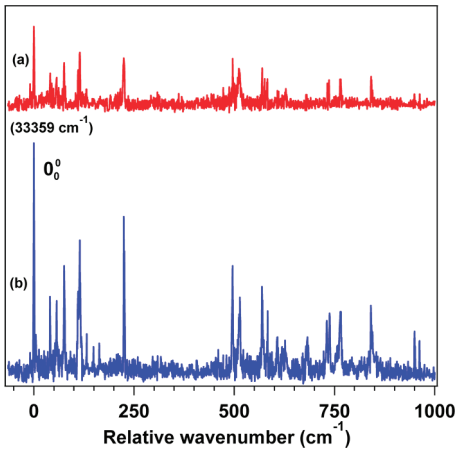

Figure 5. (a) IR-UV hole-burning spectrum by pumping the vibrational band of the 7-azaindole···2-fluoropyridine dimer at 3256 cm^{-1} and (b) one-color R2PI spectrum of the 7-azaindole···2-fluoropyridine dimer.

Table 1. BSSE and ZPE Corrected Binding Energies (kcal/mol) as well as the Relative Energies (kcal/mol) of HB1 and HB2 Structures of 7-Azaindole···2-Fluoropyridine Dimer Calculated at Various Levels of Theory[a]

	7-AI···2-FP					
	HB1			HB2		
theory	ΔE_e	ΔE_o	E_{rel}	ΔE_e	ΔE_o	E_{rel}
B3LYP/6-311++G(d,p)	−7.28	−6.38	0.00	−4.39	−3.72	2.69
B3LYP/aVDZ	−7.03	−5.94	0.00	−4.04	−3.18	2.76
PW91/6-311++G(d,p)	−6.74	−5.89	0.00	−3.49	−2.89	3.00
PW91/aVDZ	−6.49	−5.43	0.00	−3.15	−2.35	3.53
M05−2X/6-311++G(d,p)	−8.62	−7.84	0.00	−5.64	−5.04	2.80
M05−2X/aVDZ	−8.13	−7.15	0.00	−5.12	−4.34	3.16

[a] ΔE_e: BSSE corrected binding energy; ΔE_0: BSSE + ZPE corrected binding energy; E_{rel}: ZPE corrected relative energy of the conformer with respect to the most stable conformer.

Identical IR spectra by probing most of the electronic transitions in the R2PI spectrum of the dimer indicate the presence of only HB1 structure of the dimer in the experiment.

3.3. UV−UV and IR−UV Hole-Burning Spectra. To confirm whether only one conformer of the dimer is present in the experiment, UV−UV and IR−UV hole-burning spectroscopy have been performed. Figure 4b shows UV−UV hole-burning spectrum by probing the electronic origin band of the dimer at 33 359 cm^{-1} and scanning the whole R2PI spectral region of the dimer using another UV laser. R2PI spectrum of the dimer has been shown in Figure 4a for comparison with the spectrum in Figure 4b. UV−UV hole-burning spectrum shows the presence of dip in ion signal for all the electronic transitions in the R2PI spectrum of the dimer. This confirms that all the bands in the R2PI spectrum are due to presence of HB1 dimer only.

Figure 5a shows IR-UV hole-burning spectrum by probing the N−H stretching vibration of the HB1 dimer at 3256 cm^{-1}. Figure 5b again shows R2PI spectrum of the dimer for comparison with the spectrum in Figure 5a. Like UV−UV hole-burning

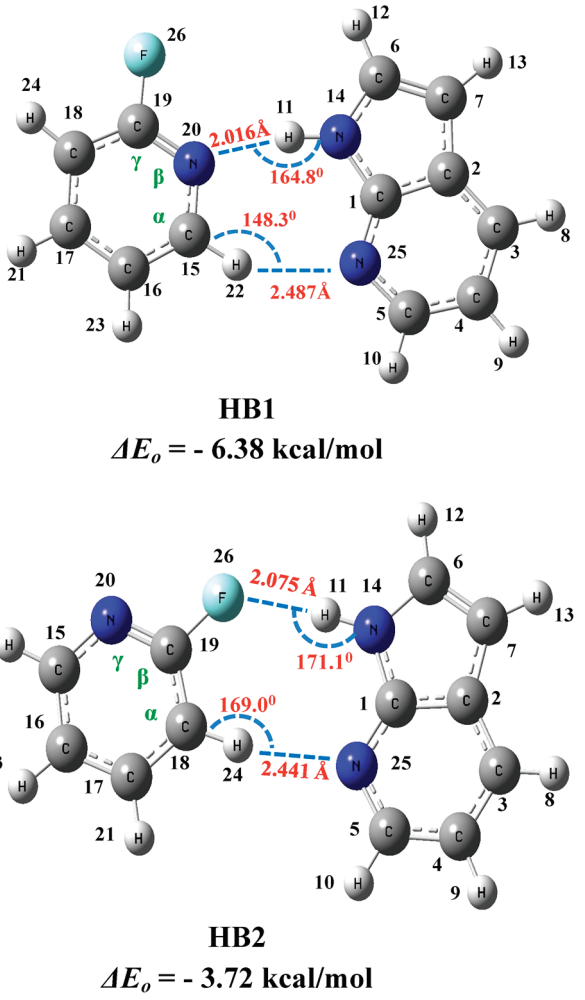

Figure 6. B3LYP/6-311++G(d,p) level optimized structures of HB1 and HB2 conformers of the 7-azaindole···2-fluoropyridine dimer. The symbols α, β, and γ in the structures are put with respect to the hydrogen bonded C−H group of 2-fluoropyridine. ΔE_0 stands for BSSE + ZPE corrected binding energy of the dimer.

spectrum, this spectrum also shows depletion in intensity of all the electronic bands in the R2PI spectrum of the dimer. Thus IR−UV hole-burning spectrum reconfirms the presence of only HB1 dimer in the experiment.

3.4. Theoretical Results. *3.4.1. Geometry of the 7-Azaindole···2-Fluoropyridine Dimer.* Two probable double-hydrogen bonded structures of the dimer in the ground electronic state are optimized at the DFT level employing various functionals B3LYP, PW91, and M05-2X using 6-311++G(d,p) and aVDZ basis sets. Figure 6 shows structures of the two conformers of the dimer optimized at the B3LYP/6-311++G(d,p) level of theory. Both of the conformers of the dimer have a planar cyclic double-hydrogen bonded structure. One of the structures is named as HB1 having N−H···N and C−H···N interactions and the other one is called as HB2 consisting of N−H···F and C−H···N interactions. The BSSE and zero point energy (ZPE) corrected binding energies as well as the relative energies of HB1and HB2 structures of the dimer calculated at various levels of theory have been provided in Table 1. Comparison of binding energies of the conformers at various levels of theory shows that HB1 is the most stable structure of the dimer. It has also been found that

Table 2. Geometrical Parameters of HB1 and HB2 Structures of 7-Azaindole···2-Fluoropyridine Dimer Calculated at the B3LYP/6-311++G(d,p) Level of Theory[a]

	7-AI···2-FP	
	HB1	HB2
$d_{N\text{-}H\cdots N}$ (Å)	2.016	
$d_{N\cdots N}$ (Å)	3.014	
Δr_{N-H}(Å)	0.015	0.0032
<N−H···N	164.8°	
$d_{N-H\cdots F}$ (Å)		2.075
$d_{N\cdots F}$ (Å)		3.077
<N−H···F		171.15°
$d_{C-H\cdots N}$ (Å)	2.487	2.441
$d_{C\cdots N}$ (Å)	3.459	3.512
Δr_{C-H}(Å)	0.0015	0.0002
<C−H···N	148.3°	169.0°
$<C_1N_{14}N_{20}C_{15}$	0.0000°	
$<C_1N_{25}C_{15}N_{20}$	0.0032°	
$<C_1N_{14}C_{19}C_{18}$		−0.0485°
$<C_{19}C_{18}N_{25}C_1$		−0.4665°

[a] For atom numbering, refer to Figure 6.

Table 3. Selected NBO Parameters of HB1 and HB2 Structures of 7-AI···2-FP Dimer Calculated at the B3LYP/aVDZ Level of Theory[a]

	7-AI···2-FP	
NBO parameters	HB1	HB2
$\Delta q(H)_{7\text{-AI}}$	0.022	0.014
$\Delta q(H)_{2\text{-FP}}$	0.032	0.025
$\Delta q(N)_{7\text{-AI}}$	−0.018	−0.019
$\Delta q(F)$	0.001	−0.021
$\Delta q(N)_{2\text{-FP}}$	−0.043	0.002
$\delta(n(N))_{2\text{-FP}}$	1.878	1.895
$\delta(n(F))_{2\text{-FP}}$	1.989	1.987
$\delta(n(N))_{7\text{-AI}}$	1.908	1.906
$\delta(\sigma^*_{NH})$	0.050	0.027
$\delta(\sigma^*_{CH})$	0.027	0.025
$E^{(2)}_{i\rightarrow j^*}(n_\sigma \rightarrow \sigma^*_{NH})$	13.13	3.98
$E^{(2)}_{i\rightarrow j^*}(n_p \rightarrow \sigma^*_{NH})$		1.56
$E^{(2)}_{i\rightarrow j^*}(n_\sigma \rightarrow \sigma^*_{CH})$	3.04	4.12

[a] $E^{(2)}_{i\rightarrow j^*}$ is in kcal/mol; all other values are in a.u.

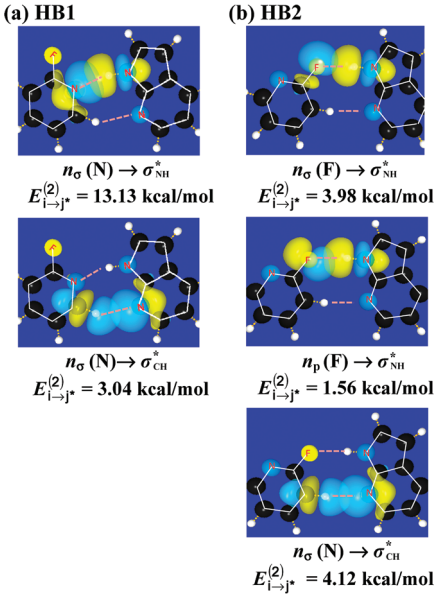

Figure 7. Natural bond orbitals of (a) HB1 and (b) HB2 conformers of 7AI···2-FP dimer showing the interactions between hydrogen bond donors and acceptors. The NBO calculations have been performed at the B3LYP/aVDZ level of theory.

relative energy of the HB2 structure is higher in energy by about 3 kcal/mol compared to that of the HB1 structure at all levels of theory.

Few important geometric parameters of HB1 and HB2 structures of the 7-AI···2-FP dimer calculated at the B3LYP/6-311++G(d,p) level of theory have been presented in Table 2. The most stable structure of the dimer, HB1, possesses a N−H···N hydrogen bond with a H···N distance of 2.016 Å as well as a C−H···N hydrogen bond with a H···N distance of 2.487 Å. On the other hand, the less stable structure of the dimer, HB2, has a similar C−H···N hydrogen bond with a H···N distance of 2.441 Å but the N−H···N hydrogen bond is replaced by N−H···F with a H···F distance of 2.075 Å. The specific dihedral angles ($<C_1N_{14}N_{20}C_{15}$, $<C_1N_{25}C_{15}N_{20}$, $<C_1N_{14}C_{19}C_{18}$, $<C_{19}C_{18}N_{25}C_1$) of the dimer listed in Table 2 point out that both HB1 and HB2 structures of the dimer are planar in the ground state.

3.4.2. NBO (Natural Bond Orbital) Analysis. It is quite interesting to compare the strength of the hydrogen bonds present in HB1 and HB2 structures of the dimer. NBO analysis is extremely significant for quantitative determination of the hydrogen bonding interaction in the X-H···A complex as the charge transfer delocalization occurs between the lone pair orbital of the hydrogen bond acceptor A and the antibonding σ^*(X-H) orbital of the donor.[66,67] The most important result obtained in the NBO calculation is the second order perturbative energy $E^{(2)}_{i\rightarrow j^*}$, where i and j* stand for a lone pair orbital and an antibonding σ^* orbital, respectively. $E^{(2)}_{i\rightarrow j^*}$ is a measure of the overlap integral between the lone pair orbital of the acceptor A and the antibonding σ^*(X-H) orbital of the donor and this is used to estimate the energy decrease caused by the electron delocalization in hydrogen bonding interaction. The results of NBO analysis for HB1 and HB2 structures of 7-AI···2-FP dimer obtained from the B3LYP/aVDZ level of calculation are listed in Table 3. The parameters $\Delta q(H)_{7\text{-AI}}$, $\Delta q(H)_{2\text{-FP}}$, $\Delta q(N)_{7\text{-AI}}$, $\Delta q(N)_{2\text{-FP}}$, and $\Delta q(F)$ in Table 3 denote atomic charges on H atom of hydrogen bond donor group of 7-AI, H atom of hydrogen bond donor group of 2-FP, N atom in the phenyl ring of 7-AI, N atom in 2-FP, and F atom of 2-FP, respectively. The electron occupancies in the lone pair orbital of N atom of 2-FP, F atom of 2-FP, and N atom of 7-AI are denoted by $\delta(n(N))_{2\text{-FP}}$, $\delta(n(F))_{2\text{-FP}}$, and $\delta(n(N))_{7\text{-AI}}$, respectively, whereas the antibonding orbitals of hydrogen bond donors N−H and C−H groups are designated as $\delta(\sigma^*_{NH})$ and $\delta(\sigma^*_{CH})$, respectively. To visualize the overlapping of the lone pair orbitals on the hydrogen bond acceptors, N atom (n_σ) or F atom (n_σ and n_p) with the antibonding orbitals of the hydrogen bond donor (σ^*_{NH} or σ^*_{CH}) in HB1 and HB2 structures of 7-AI···2-FP dimer, NBO pictures have been shown in Figure 7.

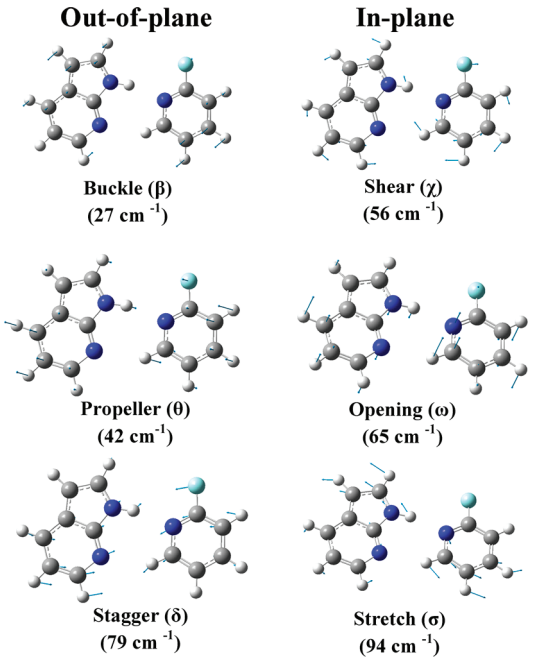

Figure 8. Normal modes of the S_1 state intermolecular vibrations of the 7-azaindole···2-fluoropyridine dimer calculated at the CIS/6-31++G(d,p) level of theory.

The comparison of the NBO parameters of HB1 and HB2 structures of the dimer presented in Table 3 clearly shows that the N−H···N interaction in the HB1 dimer is much stronger than the N−H···F interaction in the HB2 dimer. The $E^{(2)}_{i\rightarrow j^*}$ energy for $n_\sigma(N) \rightarrow \sigma^*_{NH}$ interaction in HB1 dimer is 13.13 kcal/mol, whereas $E^{(2)}_{i\rightarrow j^*}$ energies for $n_\sigma(F) \rightarrow \sigma^*_{NH}$ and $n_p(F) \rightarrow \sigma^*_{NH}$ interactions in HB2 dimer are 3.98 and 1.56 kcal/mol, respectively. The n_σ and n_p stand for the σ and p type lone pair orbitals on the hydrogen bond acceptors, respectively. The most important finding from the NBO analysis of 7-AI···2-FP dimer is that C−H···N hydrogen bonding interaction in the HB2 structure ($E^{(2)}_{i\rightarrow j^*}$ = 4.12 kcal/mol) is stronger than that in the HB1 structure ($E^{(2)}_{i\rightarrow j^*}$ = 3.04 kcal/mol). This observation can be explained in terms of the effect of electronegative substitution on the acidity of the C−H group (hydrogen bond donor) participating in the C−H···N hydrogen bond. Wetmore et al. have shown that there is substantial enhancement in the acidity of a sp^2 hybridized C−H donor upon substitution of fluorine atom at the α- as well as β-position and this leads to increase in C−H···N hydrogen bond strength.[71] In the case of the HB2 conformer of 7-AI···2-FP dimer, there is indeed a fluorine substitution at the β-position of the C−H group (see Figure 6) involving in the C−H···N hydrogen bond. On the other hand, the HB1 dimer has a fluorine substitution at the γ-position of the hydrogen bond donating C−H group (see Figure 6). Thus the acidity of the C−H donor in the HB1 dimer is less compared to that in the HB2 dimer. The activation of the C−H donor group involving C−H···O hydrogen bond is reported in the complexes of 2-pyridone and fluorobenzenes by Leutwyler and co-workers.[46] Singh et al. have also observed that C−H···N hydrogen bond is strengthened by successive fluorination of the benzene ring by studying complexes of NH_3 with a series of partially substituted fluorobenzenes.[31]

NBO analysis also demonstrates that fluorine makes hydrogen bond of intermediate strength through cooperative interaction of another hydrogen bond (C−H···N) present in the HB2 dimer although fluorine is believed to be very weak hydrogen bond acceptor. Cooperativity in hydrogen bonding interactions is defined as the strengthening of a hydrogen bond due to presence of another hydrogen bond in the neighboring site. Cooperativity effect is pronounced in the hydrogen bonded systems, where the monomer can act as a hydrogen bond donor as well as an acceptor in a concerted fashion. There are many reports in the literature on the cooperativity of the hydrogen bonding interactions in the molecular clusters.[31,46,59,72,73]

3.4.3. Inter- and Intramolecular Vibrations of the Dimer. To assign the low frequency intermolecular as well as high frequency intramolecular vibronic bands of the 7-AI···2-FP dimer observed in the R2PI spectrum, S_1 state frequency calculation of the most stable conformer of the dimer, HB1, has been performed at the CIS/6-31++G(d,p) level of the theory. The calculation predicts six low frequency intermolecular vibrational modes of the dimer and the pictures of these normal modes are provided in Figure 8. A comparison between the observed and calculated low frequency intermolecular vibrations of the dimer is also presented in Table 4. Four intermolecular modes of the dimer out of the six theoretically predicted modes are observed in the experiment. The lowest frequency out-of-plane vibration designated as buckle (β) at 27 cm^{-1} as well as in-plane opening vibration (ω) at 65 cm^{-1} do not appear in the experiment. The bands observed in the R2PI spectrum of the dimer (Figure 1b) at 40, 57, 76, and 109 cm^{-1} are assigned to out-of-plane propeller twist (θ), in-plane shear (χ), out-of-plane stagger (δ), and in-plane hydrogen bond stretching (σ) fundamental modes, respectively. The agreement between the experimentally observed and theoretically predicted intermolecular modes is excellent. The band observed at 114 cm^{-1} is assigned to the overtone transition of the shearing mode (χ) at 57 cm^{-1}. The pronounced intensity of this overtone transition could be due to Fermi resonance of two quanta of in-plane shearing vibration (57 cm^{-1}) with the in-plane stretching fundamental at 109 cm^{-1}. The band at 132 cm^{-1} is assigned to the combination of shearing (χ) and staggering (δ) fundamentals. The band at 148 cm^{-1} can be assigned to either overtone transition of the staggering fundamental or the combination of propeller twist and stretching fundamental modes. The remaining low frequency band at 163 cm^{-1} is assigned to the combination of shearing (χ) and stretching (σ) fundamentals.

As mentioned earlier in section 3.1, the observed intramolecular vibrations of 7-azaindole monomer moiety in the 7-AI··· 2-FP dimer have been assigned according to the literature report of the 7-azaindole monomer by Lin et al.[70] Experimental and CIS/6-31++G(d,p) level calculated S_1 state intramolecular vibrational frequencies of 7-azaindole moiety in 7-AI···2-FP dimer as well as 7-azaindole monomer and their assignments have been listed in Table 4. The S_1 state optimized geometry of the most stable structure of the dimer, HB1, has been provided in the Supporting Information (see Figure S1). Theoretical intramolecular vibrational frequencies of the 7-azaindole moiety in 7-AI··· 2-FP dimer and 7-azaindole monomer listed in Table 4 are scaled by a factor of 0.9066. The scaling factor has been obtained by taking the ratio of experimental (864 cm^{-1}) and calculated (953 cm^{-1}) vibrational frequencies of 22^1_0 vibration of 7-azaindole monomer. The bands observed at 225, 496, and 514 cm^{-1} in the R2PI spectrum of 7-AI···2-FP dimer are assigned as 39^2_0,

Table 4. Experimental and CIS/6-31++G(d,p) Level Calculated S_1 State Inter- and Intramolecular Vibrational Frequencies (in cm^{-1}) and Their Assignments for the 7-AI···2-FP Dimer[a]

7-AI···2-FP dimer		7-azaindole monomer		
observed	calculated	observed	calculated	assignment[b]
	27			buckle (β)
40	42			propeller twist (θ)
57	56			shear (χ)
	65			opening (ω)
76	79			stagger (δ)
109	94			stretch (σ)
114				2χ
132				$\chi + \delta$
148				2δ, $\theta + \sigma$
163				$\chi + \sigma$
225		233		39_0^2, butterfly
		280		38_0^2, ring twisting
		306		$38_0^1 39_0^1$
496	497	468	481	34_0^1, op (NCC), pyrrole
514	504	484	498	26_0^1, ip (CCC)
569				$34_0^1 + \delta$/ $26_0^1 + \chi$
583				$34_0^1 + 2\theta$/ $26_0^1 + \delta$
607				$34_0^1 + \sigma$
628				$34_0^1 + \chi + \delta$/ $26_0^1 + 2\chi$
682				$34_0^1 + \sigma + \delta$/ $26_0^1 + \chi + \sigma$
730		718		$27_0^1 38_0^1 39_0^1$
738	736	731	731	24_0^1, ip (CCC), breathing
766		756		$26_0^1 38_0^2$
841	868	864	864	22_0^1, ip (CCC)
950		932		34_0^2, γ(NCC)/$22_0^1 + \sigma$
962		962		$24_0^1 39_0^2$

[a] Experimental and calculated vibrational frequencies (in cm^{-1}) of 7-azaindole monomer are also provided in the table. Calculated intramolecular vibrational frequencies of the dimer and the monomer are scaled by a factor of 0.9066, which has been obtained by taking the ratio of experimental (864 cm^{-1}) and calculated (953 cm^{-1}) vibrational frequencies of the 22_0^1 vibration of the 7-azaindole monomer. [b] ip, in-plane bending; op, out-of-plane bending.

34_0^1, and 26_0^1 intramolecular modes of the 7-AI moiety of the dimer, respectively. The bands at 569, 583, 607, 628, and 682 cm^{-1} are assigned as intermolecular vibrations of the dimer riding on 34_0^1, and 26_0^1 intramolecular vibrations of the dimer and tentative assignments of these bands are provided in Table 4. The intramolecular vibrations $27_0^1 38_0^1 39_0^1$, 24_0^1, and $26_0^1 38_0^2$ of the 7-azaindole monomer appear in the dimer spectrum at 730, 738, and 766 cm^{-1}, respectively. The bands at 841, 950, and 962 cm^{-1} are assigned as 22_0^1, 34_0^2 or $22_0^1 + \sigma$, and $24_0^1 39_0^2$ intramolecular vibrations of the dimer, respectively.

Table 5 presents the frequencies and intensity of hydrogen bonded N−H and C−H stretching vibrations in the HB1 and HB2 structures of 7AI···2FP dimer calculated at the DFT/aVDZ level using B3LYP, PW91, and M05-2X functionals. The result shows that the performance of the B3LYP functional compared to the PW91 and M05-2X functionals is very much satisfactory to reproduce the N−H stretching frequency of the observed double hydrogen bonded planar HB1 dimer. The

Table 5. Frequency (in cm^{-1}) of Hydrogen Bonded N−H and C−H Stretching Vibrations in the HB1 and HB2 Structures of 7-AI···2-FP Dimer as well as Free C−H Stretching Vibrations of 2-Fluoropyridine (2-FP) Monomer Calculated at Various Levels of DFT[a]

		B3LYP/aVDZ		PW91/aVDZ		M05−2X/aVDZ	
HB1	$\nu_{N14-H11\cdots N20}$	3253	(1242)	3221	(1339)	3299	(1119)
	$\nu_{C15-H22\cdots N25}$	3022	(40)	3016	(49)	3029	(46)
HB2	$\nu_{N14-H11\cdots F26}$	3480	(373)	3481	(340)	3485	(405)
	$\nu_{C18-H24\cdots N25}$	3026	(107)	3021	(117)	3030	(119)
2-FP	$\nu_{C15-H22}$	3035	(10)	3035	(10)	3035	(6)
	$\nu_{C18-H24}$	3081	(1)	3083	(1)	3075	(0.1)
	$\nu_{C16-H23}$	3071	(10)	3074	(10)	3068	(3)
	$\nu_{C17-H21}$	3051	(6)	3054	(6)	3047	(4)

[a] Intensity in Km/mol is given in parentheses. Experimental N−H···N stretching frequency of HB1 conformer of 7-AI···2-FP dimer is 3256 cm^{-1}. Theoretical N−H and C−H stretching frequencies of the dimer and 2-FP monomer have been scaled by appropriate scaling factors and mentioned in detail in the text. For atom numbering, refer to Figure 6.

experimental N−H stretching frequencies of the HB1 dimer and 7-azaindole monomer are 3256 and 3521 cm^{-1}, respectively. Theoretical intensity of the N−H stretching vibration of 7-azaindole monomer is 90 km/mol. Theoretical N−H stretching frequencies are corrected using scaling factors of 0.9628, 0.9576, and 0.9432 at the B3LYP/aVDZ, PW91/aVDZ, and M05-2X/aVDZ levels, respectively. The comparison of calculated frequencies and intensity of N−H stretching vibrations in HB1, HB2 structures of the dimer strongly indicates that N−H···N hydrogen bond in HB1 is very much stronger than N−H···F bond in HB2. It is also worthwhile to compare the strength of C−H···N hydrogen bond in HB1 and HB2 structures of the dimer with the help of calculated intensity and red-shift of stretching vibration of the C−H group of 2-fluoropyridine (2-FP) involved in the hydrogen bonding. To determine the amount of red-shift in the hydrogen bonded C−H stretching frequency in HB1 and HB2 dimers, we have performed frequency calculation of 2-FP monomer. Experimental and theoretical C−H stretching vibrations of 2-fluoropyridine monomer have been reported in the literature.[74] Theoretical C−H stretching frequencies of 2-fluoropyridine monomer as well as 2-fluoropyridine moiety in the dimer are corrected using scaling factors of 0.9565, 0.9547, and 0.9356 at the B3LYP/aVDZ, PW91/aVDZ, and M05-2X/aVDZ levels, respectively. Intensity of hydrogen bonded C−H stretching vibration in HB1 and HB2 dimers calculated at the B3LYP/aVDZ level is 40 and 107 km/mol, respectively, whereas the corresponding red-shifts in the frequencies are 13 and 55 cm^{-1}. Thus it shows that C−H···N hydrogen bond in HB2 is stronger than that in the HB1 dimer, and this corroborates with the NBO analysis of the two dimeric structures described in the previous section. It is interesting to note that intensity and frequencies of non-hydrogen bonded C−H stretching vibrations in the 2-FP moiety of HB1 and HB2 dimers as well as 2-FP monomer are similar. This data also demonstrate C−H···N hydrogen bond formation in both HB1 and HB2 dimers. Experimentally, we could not obtain C−H stretching vibrations in the IR spectrum of the observed HB1 dimer probably due to their very weak intensity.

4. CONCLUSIONS

In summary, IR-UV double resonance spectroscopic techniques as well as quantum chemical calculations have been used to determine the structure of the 7-azaindole···2-fluoropyridine dimer in a supersonic jet. The electronic spectrum of the dimer obtained by excitation of the 7-azaindole moiety of the dimer using a one color R2PI method exhibits low frequency intermolecular vibrations of the dimer. It has been observed that low frequency intermolecular vibrations are also riding on the intramolecular vibration of the 7-azaindole moiety of the dimer. IR−UV and UV−UV hole burning spectroscopic techniques confirm the presence of only one conformer of the dimer in the gas phase. DFT calculations using various functionals and different basis sets predict two planar cyclic double hydrogen bonded structures of the dimer namely HB1 and HB2. Binding energy of the HB1 dimer having N−H···N and C−H···N interactions is higher by about 3 kcal/mol than that of the HB2 dimer having N−H···F and C−H···N interactions. The comparison of the RIDIR spectrum of the dimer with the theoretical IR spectra shows that the observed dimer has HB1 structure. Theoretical calculation shows that red-shifted NH stretching frequency of the HB1 dimer obtained at the DFT/B3LYP/aVDZ level compared to the DFT/PW91/aVDZ or the DFT/M05−2X/aVDZ levels matches extremely well with that of the observed dimer. There is also an excellent agreement between the experimentally observed intermolecular vibrational frequencies of the dimer in the excited electronic state with those calculated for the HB1 dimer at the CIS/6-31++G(d,p) level. NBO analysis reveals that N−H···F hydrogen bond in the HB2 dimer is weaker than N−H···N bond in HB1 dimer. It has been found that N−H···F bond is of intermediate strength with fluorine making dual hydrogen bond through a σ type and a p type lone pair orbitals although fluorine is a very weak hydrogen bond acceptor. It has also been noticed that C−H···N interaction in the HB2 dimer is stronger than that in the HB1 dimer. This is explained in terms of increase in the acidity of the hydrogen bond donating C−H group in the HB2 dimer due to fluorine substitution at the β-position of the C−H group of 2-fluoropyridine involved in the hydrogen bonding.

■ ASSOCIATED CONTENT

Supporting Information. S_1 state optimized geometry of HB1 structure of the 7-AI···2-FP dimer. This material is available free of charge via the Internet at http://pubs.acs.org.

■ AUTHOR INFORMATION

Corresponding Author

*Phone: 91-20-2590-8078. Fax: 91-20-2586-5315. E-mail: a.das@iiserpune.ac.in; aloke.das73@gmail.com.

Present Addresses

†Department of Chemistry, Scottish Church College, Kolkata-700 006, India.

■ ACKNOWLEDGMENT

The authors gratefully acknowledge the financial support received from Indian Institute of Science Education & Research (IISER), Pune to carry out the research. S.K. thanks CSIR for the research fellowship; P.B. and I.K. thank IISER Pune for their fellowships. Research support from IISER Pune supercomputer facility is also acknowledged. This work is also supported by Department of Science of Technology (Grant No. SR/S1/PC/0054/2010) and DST nanoscience unit of IISER (Project No. SR/NM/Z-3/2007). The authors wish to acknowledge Dr. Nikhil Guchhait at Calcutta University for providing access to his NBO View (Version 1.1) software package for visualization of the NBO orbitals of the hydrogen bonded dimer studied here.

■ REFERENCES

(1) Jeffrey, G. A. *An Introduction to Hydrogen Bonding*; Oxford University Press: New York, 2006.
(2) Scheiner, S. *Hydrogen bonding: A Theoretical Perspective*; Oxford University Press: New York, 1997.
(3) Desiraju, G. R.; Steiner, T. *The Weak Hydrogen Bond in Structural Chemistry and Biology*; Oxford University Press: New York, 1999.
(4) Jeffrey, G. A.; Saenger, W. *Hydrogen Bonding in Biological Structure*; Springer-Verlag: Berlin, 1991.
(5) Saenger, W. *Principles of Nucleic Acid Structure*; Springer-Verlag: New York, 1984.
(6) Burley, S. K.; Petsko, G. A. *Science* **1985**, *229*, 23.
(7) Meyer, E. A.; Castellano, R. K.; Diederich, F. *Angew. Chem., Int. Ed.* **2003**, *42*, 1210.
(8) Desiraju, G. R. *Angew. Chem., Int. Ed.* **1995**, *34*, 2311.
(9) Desiraju, G. R. *Acc. Chem. Res.* **2002**, *35*, 565.
(10) Hong, B. H.; Bae, S. C.; Lee, C.-W.; Jeong, S.; Kim, K. S. *Science* **2001**, *294*, 348.
(11) Lehn, J.-M. *Supramolecular Chemistry: Concepts and Perspectives*; VCH: New York, 1995.
(12) Steed, J. W.; Atwood, J. L. *Supramolecular Chemistry: A Concise Introduction*; Wiley: New York, 2000.
(13) Hunter, C. A. *Chem. Soc. Rev.* **1994**, *23*, 101.
(14) Hoeben, F. J. M.; Jonkheijm, P.; Meijer, E. W.; Schenning, A. P. H. J. *Chem. Rev.* **2005**, *105*, 1491.
(15) Singh, N. J.; Lee, H. M.; Suh, S. B.; Kim, K. S. *Supramol. Chem.* **2007**, *19*, 321.
(16) Zwier, T. S. *Annu. Rev. Phys. Chem.* **1996**, *47*, 205.
(17) Ebata, T.; Fujii, A.; Mikami, N. *Int. Rev. Phys. Chem.* **1998**, *17*, 331.
(18) Dessent, C. E. H.; Muller-Dethlefs, K. *Chem. Rev. (Washington, DC, U. S.)* **2000**, *100*, 3999.
(19) Matsuda, Y.; Mikami, N.; Fujii, A. *Phys. Chem. Chem. Phys.* **2009**, *11*, 1279.
(20) Dunitz, J. D.; Taylor, R. *Chem.—Eur. J.* **1997**, *3*, 89.
(21) Shimoni, L.; Glusker, J. P. *Struct. Chem.* **1994**, *5*, 383.
(22) Thalladi, V. R.; Weiss, H.-C.; Blaser, D.; Boese, R.; Nangia, A.; Desiraju, G. R. *J. Am. Chem. Soc.* **1998**, *120*, 8702.
(23) Tarakeshwar, P.; Kim, K. S.; Brutschy, B. *J. Chem. Phys.* **1999**, *110*, 8501.
(24) Buchhold, K.; Reimann, B.; Djafari, S.; Barth, H. -D.; Brutschy, B.; Tarakeshwar, P.; Kim, K. S. *J. Chem. Phys.* **2000**, *112*, 1844.
(25) Djafari, S.; Barth, H. -D.; Buchhold, K.; Brutschy, B. *J. Chem. Phys.* **1997**, *107*, 10573.
(26) Vaupel, S.; Brutschy, B.; Tarakeshwar, P.; Kim, K. S. *J. Am. Chem. Soc.* **2006**, *128*, 5416.
(27) Venkatesan, V.; Fujii, A.; Ebata, T.; Mikami, N. *Chem. Phys. Lett.* **2004**, *394*, 45.
(28) Venkatesan, V.; Fujii, A.; Ebata, T.; Mikami, N. *J. Phys. Chem. A* **2005**, *109*, 915.
(29) Venkatesan, V.; Fujii, A.; Mikami, N. *Chem. Phys. Lett.* **2005**, *409*, 57.
(30) Tonge, N. M.; MacMahon, E. C.; Pugliesi, I.; Cockett, M. C. R. *J. Chem. Phys.* **2007**, *126*, 154319.
(31) Singh, P. C.; Ray, M.; Patwari, G. N. *J. Phys. Chem. A* **2007**, *111*, 2772.
(32) Mathis, G.; Hunziker, J. *Angew. Chem., Int. Ed.* **2002**, *41*, 3203.

(33) Kopitz, H.; Zivkovic, A.; Engels, J. W.; Gohlke, H. *ChemBioChem* **2008**, *9*, 2619.
(34) Schweitzer, B. A.; Kool, E. T. *J. Org. Chem.* **1994**, *59*, 7238.
(35) Kool, E. T. *Acc. Chem. Res.* **2002**, *35*, 936.
(36) Kool, E. T. *Annu. Rev. Biochem.* **2002**, *35*, 936.
(37) Lai, J. S.; Qu., J.; Kool, E. T. *Angew. Chem., Int. Ed.* **2003**, *42*, 5973.
(38) Lai, J. S.; Kool, E. T. *J. Am. Chem. Soc.* **2004**, *126*, 3040.
(39) Moran, S.; Ren, R. X. −F.; Rumney, S., IV; Kool, E. T. *J. Am. Chem. Soc.* **1997**, *119*, 2056.
(40) Piccirilli, J. A.; Krauch, T.; Moroney, S. E.; Benner, S. A. *Nature* **1990**, *343*, 33.
(41) Evans, T. A.; Seddon, K. R. *Chem. Commun.* **1997**, 2023.
(42) Zacharias, M.; Engels, J. W. *Nucleic Acids Res.* **2004**, *32*, 6304.
(43) Pallan, P. S.; Egli, M. *J. Am. Chem. Soc.* **2009**, *131*, 12548.
(44) Anzahaee, M. Y.; Watts, J. K.; Alla, N. R.; Nicholson, A. W.; Damha, M. J. *J. Am. Chem. Soc.* **2011**, *133*, 728.
(45) Leist, R.; Frey, J. A.; Leutwyler, S. *J. Phys. Chem. A* **2006**, *110*, 4180.
(46) Frey, J. A.; Leist, R.; Leutwyler, S. *J. Phys. Chem. A* **2006**, *110*, 4188.
(47) Leist, R.; Frey, J. A.; Ottiger, P.; Frey, H. − M.; Leutwyler, S.; Bachorz, R. A.; Klopper, W. *Angew. Chem., Int. Ed.* **2007**, *46*, 7449.
(48) Taylor, C. A.; El-Bayoumi, M. A.; Kasha, M. *Proc. Natl. Acad. Sci. U.S.A.* **1969**, *63*, 253.
(49) Douhal, A.; Kim, S. K.; Zewail, A. H. *Nature* **1995**, *378*, 260.
(50) Catalan, J.; Perez, P.; del Valle, J. C.; de Paz, J. L. G.; Kasha, M. *Proc. Natl. Acad. Sci. U.S.A.* **2004**, *101*, 419.
(51) Takeuchi, S.; Tahara, T. *Proc. Natl. Acad. Sci. U.S.A.* **2007**, *104*, 5285.
(52) Fuke, K.; Yoshiuchi, H.; Kaya, K. *J. Phys. Chem.* **1984**, *88*, 5840.
(53) Fuke, K.; Yoshiuchi, H.; Kaya, K. *J. Phys. Chem.* **1989**, *93*, 614.
(54) Kim, S. K.; Bernstein, E. R. *J. Phys. Chem.* **1990**, *94*, 3531.
(55) Yokoyama, H.; Watanabe, H.; Omi, T.; Ishiuchi, S-i.; Fuji, M. *J. Phys. Chem. A* **2001**, *105*, 9366.
(56) Koizumi, Y.; Jouvet, C.; Norihiro, T.; Ishiuchi, S.; Dedonder-Lardeux, C.; Fuji, M. *J. Chem. Phys.* **2008**, *129*, 104311.
(57) Hara, A.; Sakota, K.; Nakagaki, M.; Sekiya, H. *Chem. Phys. Lett.* **2005**, *407*, 30.
(58) Brause, R.; Krugler, D.; Schmitt, M.; Kleinermanns, K.; Nakajima, A.; Miller, T. A. *J. Chem. Phys.* **2005**, *123*, 224311.
(59) Sakota, K.; Kageura, Y.; Sekiya, H. *J. Chem. Phys.* **2008**, *129*, 054303.
(60) Sekiya, H.; Sakota, K. *J. Photochem. Photobiol. C: Photochem. Rev.* **2008**, *9*, 81.
(61) Komoto, Y.; Sakota, K.; Sekiya, H. *Chem. Phys. Lett.* **2005**, *406*, 15.
(62) Hazra, M. K.; Samanta, A. K.; Chakraborty, T. *J. Phys. Chem. A* **2007**, *111*, 7813.
(63) Hazra, M. K.; Mukherjee, M.; Goswami, D.; Chakraborty, T. *Chem. Phys. Lett.* **2011**, *503*, 203.
(64) Kumar, S.; Biswas, P.; Kaul, I.; Das, A. *J. Phys. Chem. A* **2011**, *115*, 7461.
(65) Boys, S. F.; Bernardi, F. *Mol. Phys.* **1970**, *19*, 553.
(66) Weinhold, F.; Landis, C. R. *Valency and Bonding: A Natural Bond Orbital Donor-Acceptor Perspective*; Cambridge University Press: New York, 2005.
(67) Reed, A. E.; Curtiss, L. A.; Weinhold, F. *Chem. Rev. (Washington, D. C.)* **1988**, *88*, 899.
(68) *NBO 5.0*; Glendening, J., Baedwnhoop, K., Reed, A. E., Carpenter, J. E., Bohmann, J. A., Morales, C. M., Weinhold, F., Eds.; Theoretical Chemistry Institute, University of Wisconsin: Madison, WI, 2001.
(69) Frisch, M. J. et al. *Gaussian 03*, revision E.01; Gaussian, Inc.: Wallingford, CT, 2004.
(70) Lin, J. L.; Tzeng, W. B. *Chem. Phys. Lett.* **2003**, *380*, 503.
(71) Wetmore, S. D.; Schofield, R.; Smith, D. M.; Radom, L. *J. Phys. Chem. A* **2004**, *108*, 9161.
(72) Ziolkowski, M.; Grabowski, S. J.; Leszczynski, J. *J. Phys. Chem. A* **2006**, *110*, 6514.
(73) Kar, T.; Scheiner, S. *J. Phys. Chem. A* **2004**, *108*, 9161.
(74) Nibu, Y.; Marui, R.; Shimada, H. *J. Phys. Chem. A* **2006**, *110*, 9627.